Proceedings of the Institution of Civil Engineers
Water Management 162
August 2009 Issue WM4
Pages 269–277
doi: 10.1680/wama.2009.00038

Paper 800038
Received 21/02/2008
Accepted 04/08/2008

Keywords:
hydraulics & hydrodynamics/models (physical)

S. Kucukali
Assistant Professor, Division of Civil Engineering, Zonguldak Karaelmas University, Zonguldak, Turkey

H. Chanson
Professor, Division of Civil Engineering, The University of Queensland, Brisbane, Australia

ice
Institution of Civil Engineers

Turbulent length–time scales distributions in hydraulic jumps

S. Kucukali PhD and H. Chanson PhD, DEng

Air–water flow measurements were performed in hydraulic jump flows for a range of inflow Froude numbers. The experiments were conducted in a large-sized facility using phase-detection intrusive probes. The void fraction measurements showed the presence of an advective diffusion shear layer where the air concentration vertical distributions were successfully compared with an analytical solution of the advective diffusion equation for air bubbles. In the air–water shear layer, a new empirical relationship between the maximum air concentration decay as a function of both the distance from the jump toe and the inflow Froude number was derived. Air–water turbulent time and length scales were deduced from auto- and cross-correlation analyses based on the method of Chanson (2007). The result provided some characteristic transverse time and length scales of the eddy structures advecting the air bubbles in the developing shear layer. The turbulence time scale data showed an increase with the relative elevation above the bed, as well as some decrease with increasing distance from the toe. The dimensionless integral turbulent length scale L_{xz}/d_1 was closely related to the inflow depth.

NOTATION

C	air concentration defined as the volume of air per unit volume of water
C_{max}	maximum void fraction in the air bubble diffusion layer
D_t	turbulent diffusivity (m^2/s) of air bubbles in the air–water flow
D'_t	turbulent diffusivity (m^2/s) of air bubbles in the interfacial free-surface flow
$D^\#$	dimensionless turbulent diffusivity: $D^\# = D_t/(U_1 \times d_1)$
d_1	flow depth (m) measured immediately upstream of the hydraulic jump
d_2	flow depth (m) measured immediately downstream of the hydraulic jump
Fr_1	upstream Froude number: $Fr_1 = U_1/(\sqrt{g \times d_1})$
g	gravity constant: $g = 9{\cdot}80\ m/s^2$ in Brisbane, Australia
L_j	hydraulic jump length (m)
L_{xz}	transverse air–water length scale (m): $L_{xz} = \int_{z=0}^{z=z((R_{xz})_{max}=0)} (R_{xz})_{max} \times d\tau$
Q	water discharge (m^3/s)
Re	Reynolds number: $Re = (U_1 \times d_1)/\nu$
R_{xx}	normalised auto-correlation function (reference probe)
R_{xz}	normalised cross-correlation function between two probe output signals
$(R_{xz})_{max}$	maximum cross-correlation between two probe output signals
T_{xx}	auto-correlation integral time scale: $T_{xx} = \int_{\tau=0}^{\upsilon=\tau(R_{xx}=0)} R_{xx} \times d\tau$
T_{xz}	cross-correlation integral time scale: $T_{xz} = \int_{\tau=\tau[R_{xz}=(R_{xz})_{max}]}^{\upsilon=\tau(R_{xz}=0)} R_{xz} \times d\tau$
W	channel width (m)
x	longitudinal distance from the sluice gate (m)
x_1	longitudinal distance from the gate to the jump toe (m)
$Y_{C_{max}}$	distance (m) normal to the jet support where $C = C_{max}$
y	distance (m) measured normal to the channel bed
z	transverse distance (m) from the channel centreline
z_{max}	transverse distance (m) where the cross-correlation coefficient tends to zero
ν	kinematic viscosity of water (m^2/s)
τ	time lag (s)

1. INTRODUCTION

A hydraulic jump is the transition from a supercritical regime to a subcritical regime and it is characterised by a highly turbulent flow, macro-scale vortices, a lot of kinetic energy dissipation and a bubbly two-phase flow (Figure 1). It is often characterised by its inflow Froude number Fr_1 defined as

$$Fr_1 = \frac{U_1}{\sqrt{g \times d_1}} \quad (1)$$

where U_1 is the depth-averaged upstream flow velocity, d_1 is the upstream flow depth and g is the acceleration of gravity (Figure 1).

In a hydraulic jump flow, the free-surface disturbances and vortex flow induce some air entrainment. The air entrainment has important implications for oxygen transfer. Air concentration measurements in hydraulic jumps were first studied by Rajaratnam[1] who showed some influence of the Froude number on the bubbly flow structure. Resch *et al.*[2] demonstrated that the air concentration profiles have different shapes depending on the upstream flow conditions. Rajaratnam[1] and Chanson[3] measured the maximum air concentration at the jump mixing layer, and Chanson and Brattberg[4] showed that the maximum air concentration exhibited a longitudinal decay.

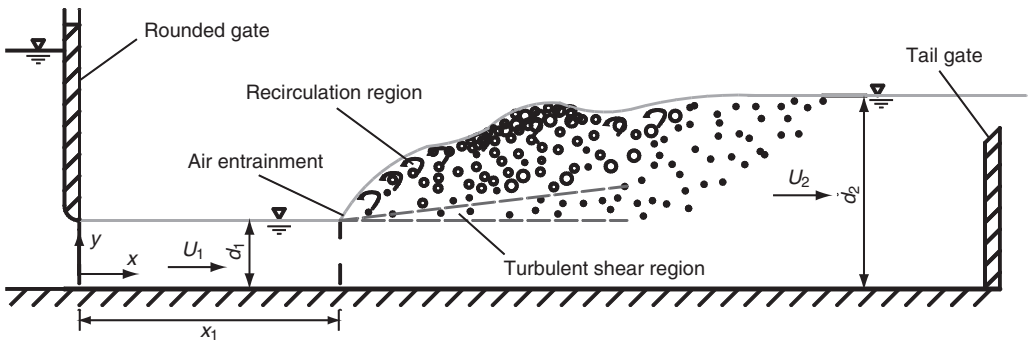

Figure 1. Schematic diagram of the hydraulic jump flow characteristics

Mouaze *et al.*,[5] Long *et al.*[6] and Chanson[7,8] related the turbulent length scales in hydraulics jumps with the upstream flow depths by using different measuring techniques. Table 1 summarises the recent experimental investigations of air entrainment in hydraulic jumps. The table illustrates the range of low inflow Froude numbers investigated by Murzyn *et al.*[9] and the two Froude numbers studied by Chanson and Brattberg.[4] The study by Chanson[7] covered some large Froude numbers and yielded air–water turbulent length scales. The aim of this study is to examine in detail the distributions of turbulent length and time scales and the air concentration profiles in hydraulic jumps with large inflow Froude numbers.

2. EXPERIMENTAL SET-UP AND METHODOLOGY

The experiments were carried out in a horizontal rectangular flume 0·50 m wide, 0·45 m deep with 3·2 m long glass sidewalls and a polyvinyl chloride bed at the University of Queensland (Figure 2). The channel was previously used by Chanson.[7] The water discharge was measured with a Venturi meter located in the supply line; the meter was calibrated with a large V-notch weir. The discharge measurement was accurate within ±2%. The clear-water flow depths were measured using rail-mounted point gauges with a 0·2 mm accuracy.

The air–water flow properties were measured with two single type conductivity probes (diameter 0·35 mm) as previously used by Chanson and Carosi.[10] The working principle of the conductivity probe relies on the difference in electrical resistance between air and water.[11,12] The probes were excited by an electronic system (reference number UQ82.518) designed with a response time of less than 10 μs. During the experiments, each conductivity probe sensor was sampled at 10 kHz for 48 s.

Reference	Flow conditions	Measurement technique(s)	Comments
Chanson and Brattberg[4]	$Fr_1 = 6{\cdot}33$ and 8·48 $Re = 3{\cdot}3 \times 10^4$–$4{\cdot}4 \times 10^4$ $U_1 = 2{\cdot}34$ and 3·14 m/s $d_1 = 0{\cdot}014$ m $x_1 = 0{\cdot}50$ m	Pitot tube: 3·3 mm external dia. Conductivity probe (double tip, 0·025 mm inner electrode, 8 mm tip spacing)	$W = 0{\cdot}25$ m
Murzyn *et al.*[9]	$Fr_1 = 2{\cdot}0$–4·8 $Re = 4{\cdot}6 \times 10^4$–$8{\cdot}8 \times 10^4$ $U_1 = 1{\cdot}50$–2·19 m/s $d_1 = 0{\cdot}021$ to 0·059 m	Optical fibre probe (double tip, 0·010 mm dia., 1 mm tip spacing)	$W = 0{\cdot}3$ m
Chanson[7]	$Fr_1 = 5{\cdot}0$–8·4 $Re = 2{\cdot}5 \times 10^4$–$9{\cdot}5 \times 10^4$ $U_1 = 1{\cdot}85$ to 3·9 m/s $d_1 = 0{\cdot}013$–0·029 m $x_1 = 0{\cdot}5$ and 1·0 m P/D inflow conditions $Fr_1 = 5{\cdot}1$ and 8·6 $Re = 6{\cdot}8 \times 10^4$–$9{\cdot}8 \times 10^4$ $U_1 = 2{\cdot}6$ and 4·15 m/s $d_1 = 0{\cdot}026$ and 0·024 m P/D inflow conditions	Conductivity probes (single tip, 0·35 mm inner electrode)	$W = 0{\cdot}25$ m $W = 0{\cdot}50$ m
Present study	$Fr_1 = 4{\cdot}7$–6·9 $Re = 5 \times 10^4$–8×10^4 $U_1 = 2{\cdot}28$–3·35 m/s $d_1 = 0{\cdot}024$ m $x_1 = 1{\cdot}0$ m P/D inflow conditions	Conductivity probes (single tip, 0·35 mm inner electrode)	$W = 0{\cdot}50$ m

Table 1. Recent experimental investigations of air entrainment in hydraulic jumps (F/D indicates fully developed, P/D indicates partially developed)

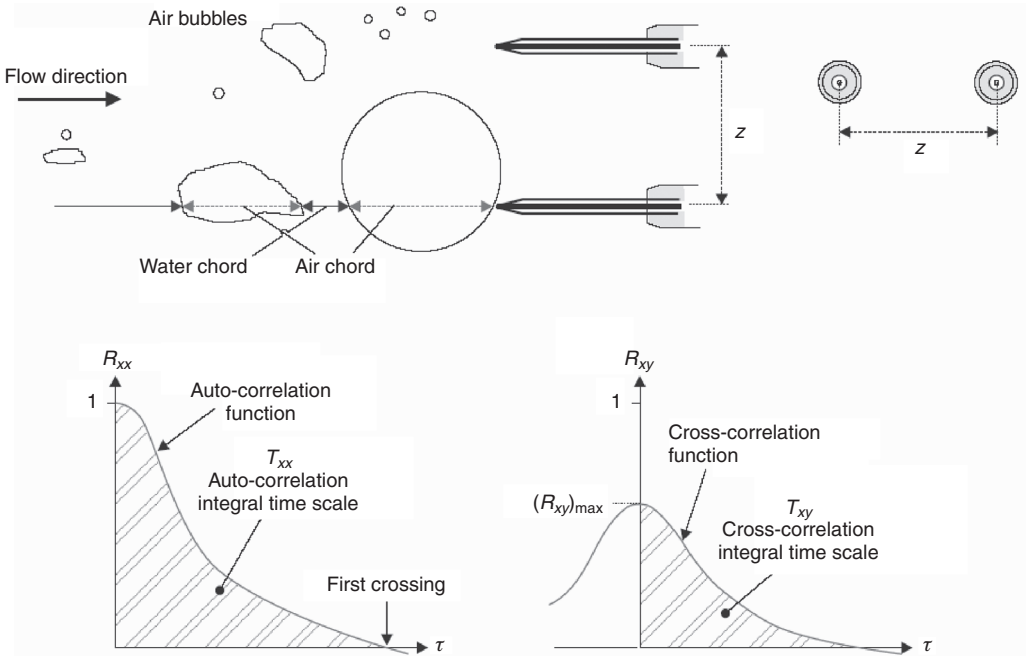

Figure 2. Sketch of auto- and cross-correlation functions for two identical single-tip conductivity probes separated by a transverse distance

The probe displacement in the vertical direction was controlled by a fine adjustment system connected to a Mitutoyo™ digimatic scale unit with a vertical accuracy Δy of less than 0·1 mm. With two single-tip probes, the reference conductivity probe was located on the channel centreline ($z = 0$) while the second identical probe was separated in the transverse direction by a known spacing z using the method employed by Chanson[7] (Figure 2). Both probe sensors were located at the same vertical and stream-wise distances y and x, respectively.

The air–water flow measurements were performed for: $Fr_1 = 4{\cdot}7$, 5·8 and 6·9 (Table 1). The jump toe location was controlled by an upstream rounded gate and by a downstream overshoot gate; where x is the longitudinal distance from the sluice gate, and x_1 is the distance from the gate to the jump toe (Figure 1). The air–water flow properties were measured downstream of the jump toe in the developing air–water flow region: that is $(x - x_1)/d_1 < 25$ where the upstream depth d_1 was measured typically 10–20 cm upstream of the jump toe. The flow conditions are summarised in Table 2, where Q is the water discharge, d_2 is the downstream conjugate depth, L_j is the measured jump length and Re is the inflow Reynolds number defined as

$$Re = \frac{U_1 \times d_1}{\nu} \quad (2)$$

where ν is the kinematic viscosity of water. All the experiments were carried out with the same inflow depth ($d_1 = 0{\cdot}024$ m) and the same distance from the upstream gate ($x_1 = 1$ m). The inflow was characterised by a partially developed boundary layer ($\delta/d_1 \sim 0{\cdot}4$–$0{\cdot}6$). Full details of the data sets are reported by Kucukali and Chanson.[13]

2.1. Signal processing of the conductivity probes

The air–water flow properties were calculated using a single threshold technique and the threshold was set at about 45–55% of the air–water voltage range (error <1% on void fraction). The basic probe outputs were the air concentration or void fraction C. When two single-tip probes were simultaneously sampled, the correlation analysis results included the maximum cross-correlation coefficient $(R_{xz})_{max}$, and the integral time scales T_{xx} and T_{xz} where

$$T_{xx} = \int_{\tau=0}^{\upsilon=\tau(R_{xx}=0)} R_{xx} \times d\tau \quad (3)$$

$$T_{xz} = \int_{\tau=\tau(R_{xz}=(R_{xz})_{max})}^{\upsilon=\tau(R_{xz}=0)} R_{xz} \times d\tau \quad (4)$$

with τ being the time lag, R_{xx} being the normalised auto-correlation function of the reference probe signal and R_{xz} being the normalised cross-correlation function between the two probe signals. T_{xx} represents an integral time scale of the longitudinal bubbly flow structures (see Figure 6 later, in

x_1: m	d_1: m	Q: m^3/s	d_2: m	L_j: m	U_1: m/s	Re	Fr_1
1·0	0·024	0·0273	0·150	0·50	2·28	5×10^4	4·7
1·0	0·024	0·0337	0·192	0·62	2·81	7×10^4	5·8
1·0	0·024	0·0402	0·230	0·80	3·35	8×10^4	6·9

Table 2. Experimental flow conditions

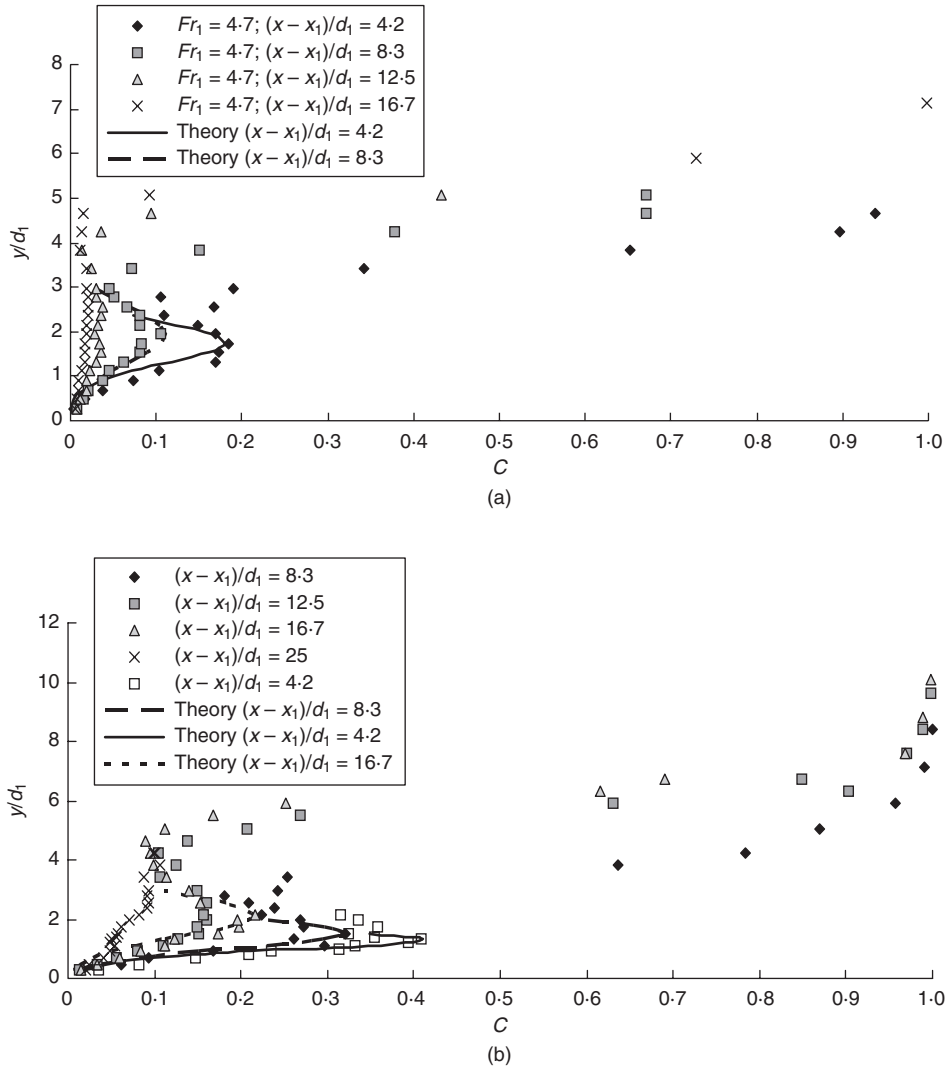

Figure 3. Dimensionless distributions of void fraction along the hydraulic jump, comparison with Equation 6 in the shear layer: (a) $Fr_1 = 4{\cdot}7$; (b) $Fr_1 = 6{\cdot}9$

Section 3). It is a characteristic time of the large eddies advecting the air–water interfaces in the longitudinal direction. T_{xz} is a characteristic time scale of the vortices with a transverse length scale z.[7] When some identical experiments were repeated with different transverse spacing z, a characteristic integral length scale was calculated as

$$L_{xz} = \int_{z=0}^{z=z((R_{xz})_{max}=0)} (R_{xz})_{max} \times d\tau \quad (5)$$

The length scale L_{xz} represented a transverse length scale of the large vortical structures advecting the air bubbles in the hydraulic jump flow.[7,10] First it must be stressed that the analysis could be performed only at locations where correlation calculations were meaningful. In some regions and at some sampling locations, the calculations were unsuccessful. The present results showed negligible cross-correlations for $z/d_1 > 0{\cdot}6$. Herein most calculations were performed by hand and all meaningless results were rejected. The basic correlation results included the maximum cross-correlation coefficient $(R_{xz})_{max}$ for several transverse spacings z with identical flow conditions and at identical locations, the auto- and cross-correlation time scales T_{xx} and T_{xz}, and the transverse air–water length scale z, which was then calculated using Equation 5 between $z = 0$ and $z_{max} = 27{\cdot}5$ mm. For larger transverse distances, the correlations calculations were unsuccessful.

3. EXPERIMENTAL RESULTS AND DISCUSSION

In the hydraulic jump flow, the air concentration profiles showed consistently two distinct regions

(*a*) the turbulent shear region
(*b*) the upper region.

In hydraulic jump flows, air entrainment occurs in the form of air bubbles and air packets entrapped at the impingement of the upstream jet flow with the roller (Figure 1). Typical air concentration distributions along the hydraulic jump for different Froude numbers are shown in Figure 3.

Figure 3 presents the vertical distributions of void fraction C as a function of the dimensionless distance above the invert y/d_1 at several dimensionless distances from the jump toe $(x - x_1)/d_1$. In the turbulent shear layer, the air concentration distributions

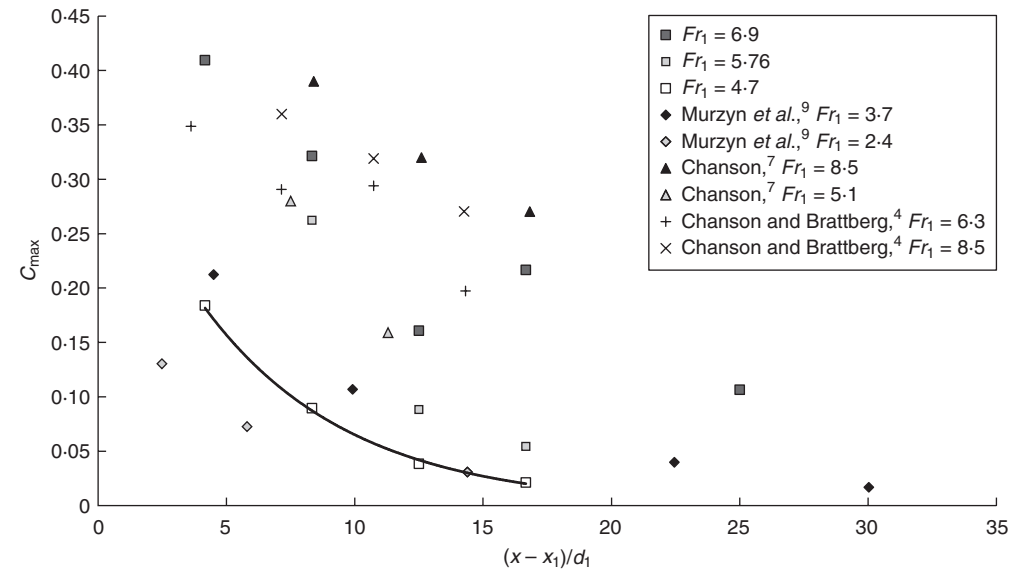

Figure 4. Longitudinal distribution of maximum void fraction C_{max} in the shear layer of hydraulic jumps for several inflow Froude numbers: comparison between the present data set ($Fr_1 = 4{\cdot}7$, 5·8 and 6·9), the data of Chanson and Brattberg,[4] Murzyn *et al.*[9] and Chanson,[7] and Equation 7 for $Fr_1 = 4{\cdot}7$

followed a Gaussian distribution first proposed by Chanson[14]

$$C = C_{max} \times \exp\left\{-\frac{[(y - Y_{C_{max}})/d_1]^2}{4 \times D^{\#} \times (x - x_1)/d_1}\right\} \quad (6)$$

where $Y_{C_{maz}}$ is the vertical elevation of the maximum air content C_{max}, $D^{\#} = D_t/(U_1 \times d_1)$, D_t is the turbulent diffusivity which averages the effects of turbulent diffusion of longitudinal velocity gradient, x and y are the longitudinal and vertical distances measured from the channel intake and bed respectively. Equation 6 is valid for hydraulic jumps with partially developed inflow conditions and it was validated with several data sets.[2,4,6,7] The effect of buoyancy is a slight shift upwards of the air bubble advective diffusion layer. In practice, Equation 6 provides good agreement with experimental data in the advective diffusion region of hydraulic jumps with partially developed inflow conditions.

The void fraction profiles showed some marked difference between the mixing layer zone (Equation 6) and the upper flow region. At large Froude numbers, the experimental results showed that the entrained air was more thoroughly dispersed, and it remained submerged for a greater distance (e.g. Figure 3). A comparison between Figures 3(a) and 3(b) suggests that both the maximum void fractions and the length of the air–water shear layer increased with increasing inflow Froude numbers. The finding is in agreement with the work of Gualtieri and Chanson[15] in a smaller channel. In the air–water mixing layer, the maximum void fraction C_{max} decreased with increasing distance from the jump toe (Figure 4). The present data are compared with other data sets in Figure 4 and they were best correlated by

$$C_{max} = 0{\cdot}07 \times Fr_1 \times \exp\left(-0{\cdot}064 \times \frac{x - x_1}{d_1}\right) \quad \text{for } 2{\cdot}4 \leqslant Fr_1 \leqslant 8{\cdot}5 \quad (7)$$

with a correlation coefficient of 0·82. Equation 7 is shown in Figure 4. The vertical elevation of the maximum void fraction $Y_{C_{max}}/d_1$ in the shear region increased along the hydraulic jump (Figure 5). It is suggested that this might result from buoyancy effects. Further the experimental observations showed that elevation of maximum bubble count rate $Y_{F_{max}}$ was always located below the $Y_{C_{max}}$ (i.e. $Y_{F_{max}} < Y_{C_{max}}$). The finding is consistent with the earlier data of Chanson and Brattberg,[4] Murzyn *et al.*[9] and Chanson.[7] Chanson[7] argued that the finding was related to a double diffusion process where vorticity and air bubbles diffuse at a different rate and in a different manner downstream of the impingement point.

Some distributions of auto-correlation time scales are presented in Figure 6. Note that the void fraction profiles are also shown, and that the auto-correlation time scales T_{xx} are shown in dimensional units (ms) with a logarithmic scale (bottom horizontal axis). The cross-correlation time scale T_{xz} is a time scale of transverse connection between the air–water flow structures as seen by two probes separated by a distance z. As can be seen from Figure 6, the turbulent time scales increased towards the free surface and decreased along the hydraulic jump, as did the air concentration. The time scales were within the range of 1 to 100 ms and the results were in agreement with the earlier results of Chanson.[7]

In Figure 7, some effect of the separation distance z on the cross-correlation time scales can be seen. For example, for $Fr_1 = 4{\cdot}7$, $(x - x_1) = 0{\cdot}1$ m and $y/d_1 = 1{\cdot}1$ point, T_{xz} decreased from 4·39 to 1·24 ms for $z = 3{\cdot}7$ to 27·5 mm. Figure 7 presents typical vertical distributions of auto- and cross-correlation time scales. The data showed systematically that the auto-correlation time scales T_{xx} were larger than the cross-correlation time scales T_{xz} (Figure 7). The auto-correlation time scale T_{xx} represents a rough measure of the longest longitudinal connection in the air–water flow structures.

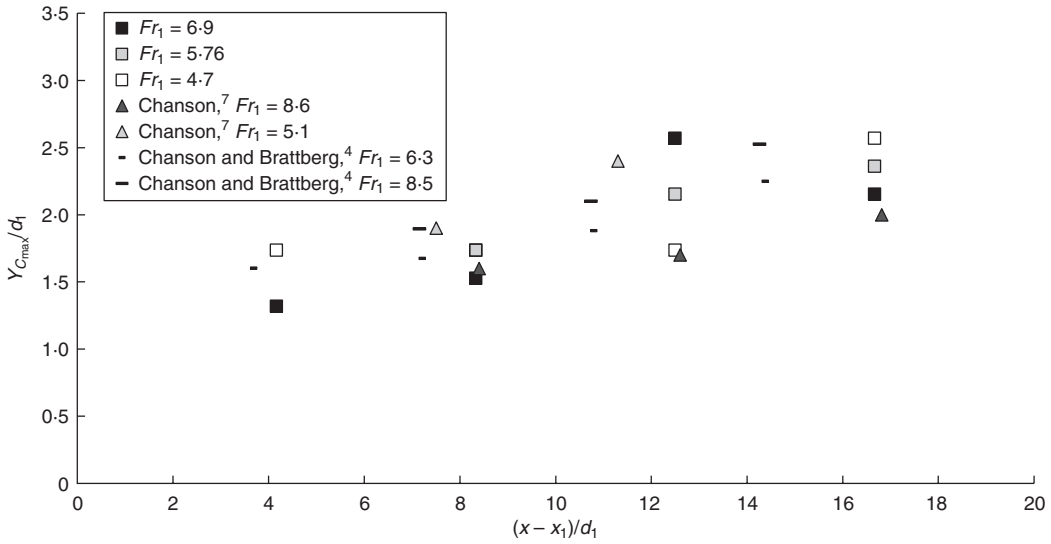

Figure 5. Location of the maximum air concentration in the hydraulic jump for various Fr_1 numbers

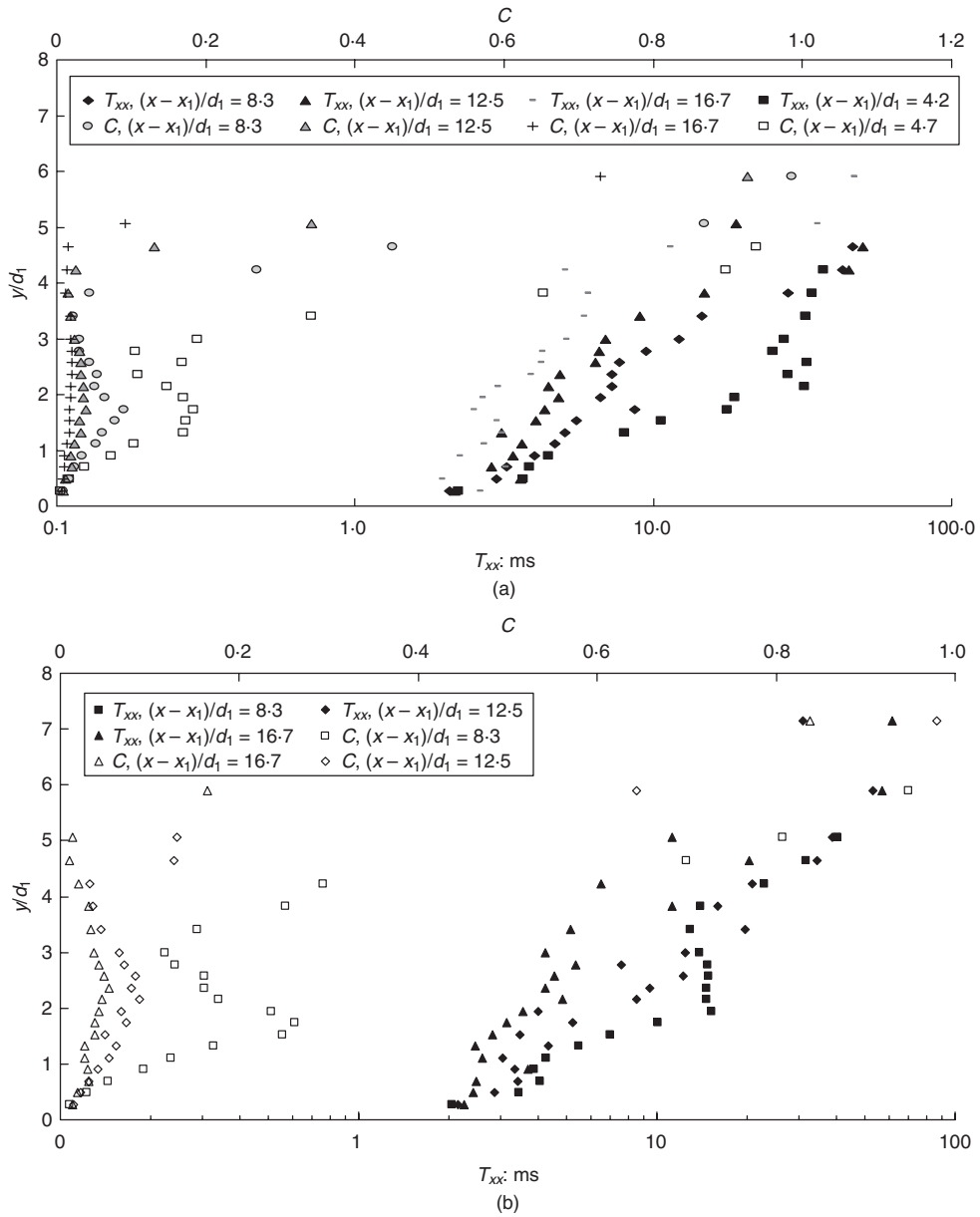

Figure 6. Vertical distribution of auto-correlation time scale T_{xx} along the hydraulic jump: (a) $Fr_1 = 4{\cdot}7$; (b) $Fr_1 = 5{\cdot}8$

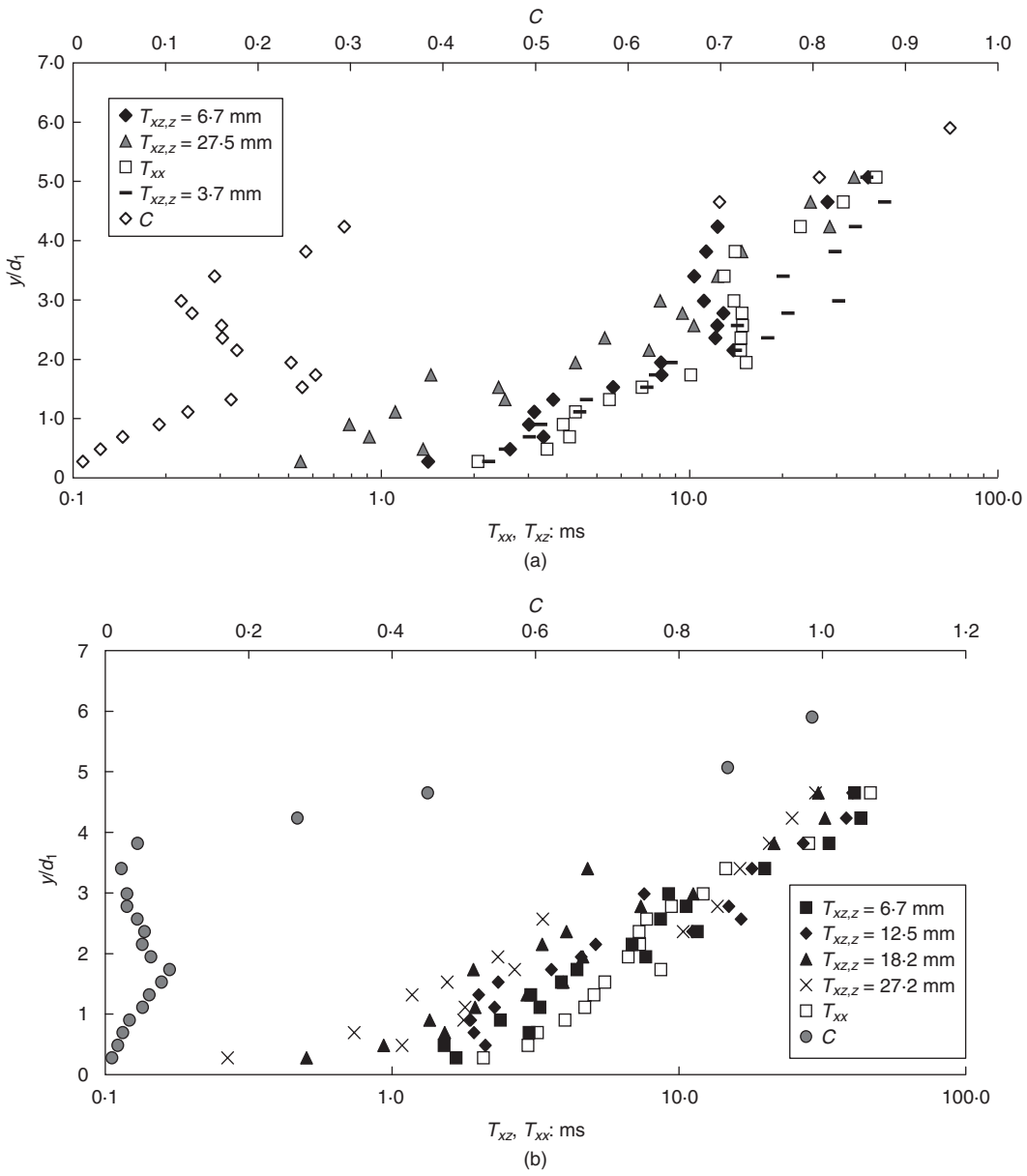

Figure 7. Vertical distribution of auto-correlation and cross-correlation time scales T_{xx} and T_{xz} for different transverse distances at $(x - x_1)/d_1 = 8{\cdot}3$: (a) $Fr_1 = 4{\cdot}7$; (b) $Fr_1 = 5{\cdot}8$

The length scale L_{xz} is an integral air–water turbulence length scale which characterised the transverse size of the large vortical structures advecting the air bubbles in the hydraulic jump flows. It was a function of the inflow conditions, of the streamwise position $(x - x_1)/d_1$ and vertical elevation y/d_1. Typical dimensionless distributions of integral length scales L_{xz}/d_1 are presented in Figures 8 and 9. The void fraction distributions are also shown for completeness. Figures 8 and 9 illustrate some effect of the vertical elevation y/d_1 on the integral air–water turbulent length scale. Typically the integral length scale L_{xz} increased with increasing distance from the channel bed, and the dimensionless integral turbulent length scale L_{xz}/d_1 was typically between 0·2 and 0·8. They suggested further some correlation between the void fraction and the integral length scale L_{xz}.

Based on the present study and the data of Chanson,[7] L_{xz} increases with y/d_1 (Figure 10). The data suggested that turbulent length scale closely related with the flow depth in the turbulent shear region and was best fitted by

$$\frac{L_{xz}}{d_1} = 0{\cdot}13 \times \frac{y}{d_1} + 0{\cdot}08 \quad \text{for } 0{\cdot}3 \leqslant y/d_1 \leqslant 5 \tag{8}$$

with a correlation coefficient of 0·88. Equation 8 might suggest that the macro-scale vortices enlarge in transverse size towards the free surface.

The integral length scale results were consistent with the study by Chanson,[7,8] but some differences were observed compared with the findings of Mouaze *et al.*[6] The latter study, however, recorded only free-surface turbulence length scales.

4. CONCLUSION

New air–water flow measurements were performed in partially developed hydraulic jump flows for a range of inflow Froude numbers. The void fraction measurements showed the presence of an advective diffusion shear layer in which the void fractions

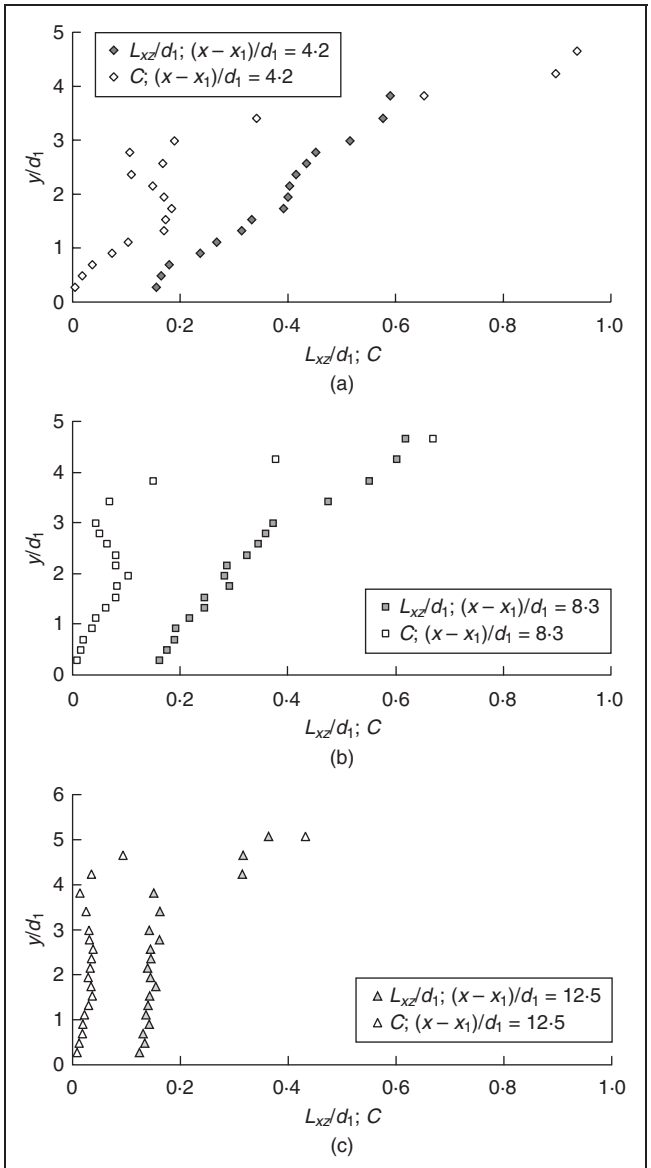

Figure 8. Distribution of dimensionless air–water transverse length scales L_{xz}/d_1 in a hydraulic jump, $Fr_1 = 4{\cdot}7$: (a) $(x - x_1)/d_1 = 4{\cdot}2$; (b) $(x - x_1)/d_1 = 8{\cdot}3$; (c) $(x - x_1)/d_1 = 12{\cdot}5$

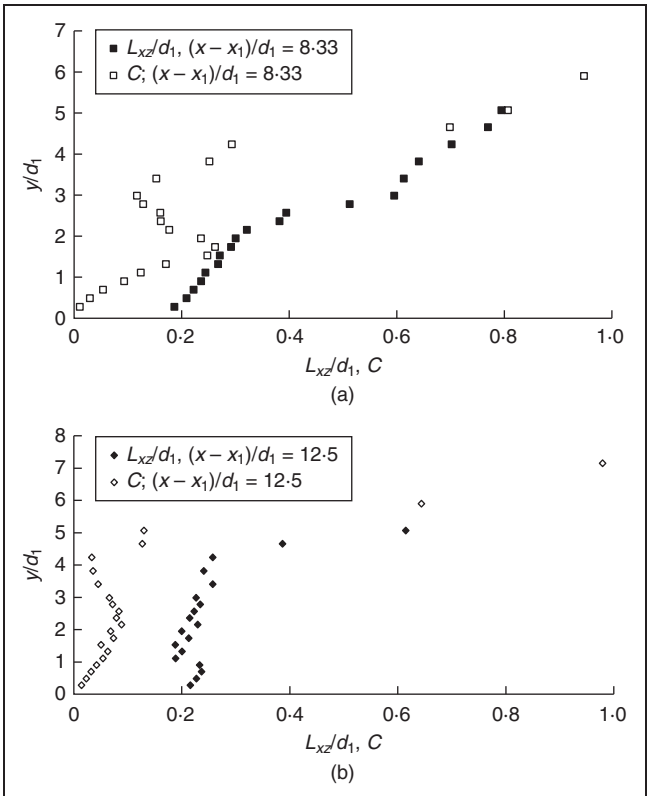

Figure 9. Distribution of dimensionless air–water transverse length scales L_{xz}/d_1 in a hydraulic jump, $Fr_1 = 5{\cdot}8$: (a) $(x - x_1)/d_1 = 8{\cdot}3$; (b) $(x - x_1)/d_1 = 12{\cdot}5$

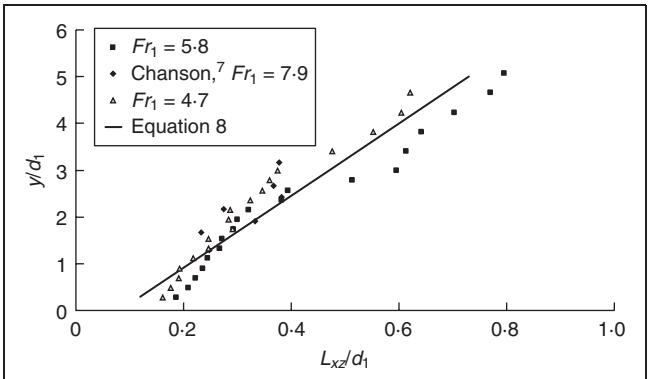

Figure 10. Distribution of dimensionless air–water transverse length scales L_{xz}/d_1 in a hydraulic jump for various Fr_1 numbers at $x - x_1 = 0{\cdot}2$ m

profiles matched closely an analytical solution of the advective diffusion equation for air bubbles. Similar earlier results were observed in plunging jet flows and hydraulic jumps. In the air–water shear layer, the maximum void fraction C_{max} decreased with increasing distance from the jump toe. The data suggest that both the maximum void fractions and the length of the air–water shear layer increased with increasing inflow Froude numbers.

Air–water turbulent time and length scales were deduced from auto- and cross-correlation analyses based on the method of Chanson.[7,8] The result provided some characteristic transverse time and length scales of the eddy structures advecting the air bubbles in the developing shear layer. The results showed the auto-correlation time scales T_{xx} were larger than the transverse cross-correlation time scales T_{xz}, which were in the range 1–100 ms. The dimensionless turbulent integral length scale L_{xz}/d_1 was closely related to the inflow depth: that is $L_{xz}/d_1 = 0{\cdot}2$–$0{\cdot}8$, with L_{xz} increasing towards the free surface.

The authors believe that the present results bring a fresh perspective towards better understanding of hydraulic jump flows and the distributions of turbulent length and time scales.

ACKNOWLEDGEMENTS

The authors thank Graham Illidge and Clive Booth (University of Queensland) for their technical assistance. The author (SK) acknowledges the financial support of the Scientific and Technological Research Council of Turkey (TUBITAK) and the support of the division of civil engineering at the University of Queensland.

REFERENCES

1. Rajaratnam N. An experimental study of air entrainment characteristics of the hydraulic jump. *Journal of the Institution of Engineering India*, 1962, **42**, No. 7, 247–273.
2. Resch F. J., Leutheusser H. J. and Alemu S. Bubbly two-phase flow in hydraulic jump. *Journal of Hydraulic Engineering,* 1974, **100**, No. 1, 137–149.
3. Chanson H. *Air Bubble Entrainment in Free-Surface Turbulent Shear Flows*. Academic Press, London, 1997.
4. Chanson H. and Brattberg T. Experimental study of the air–water shear flow in a hydraulic jump. *International Journal of Multiphase Flow*, 2000, **26**, No. 4, 583–607.
5. Mouaze D., Murzyn F. and Chaplin J. R. Free surface length scale estimation in hydraulic jumps. *Trans. ASME, Journal of Fluids Engineering*, 2005, **127**, No. 6, 1191–1193.
6. Long D., Rajaratnam N., Steffler P. M. and Smy P. R. Structure of flow in hydraulic jumps. *Journal of Hydraulic Research*, 1991, **29**, No. 2, 207–218.
7. Chanson H. *Air Bubble Entrainment in Hydraulic Jumps. Similitude and Scale Effects*. Dept. of Civil Engineering, The University of Queensland, Brisbane, Australia, 2006, Report No. CH57/05.
8. Chanson H. Bubbly flow structure in hydraulic jump. *European Journal of Mechanics – B/Fluids*, 2007, **26**, No. 3, 367–384.
9. Murzyn F., Mouaze D. and Chaplin J. R. Optical fibre probe measurements of bubbly flow in hydraulic jumps. *International Journal of Multiphase Flow*, 2005, **31**, No. 1, 141–154.
10. Chanson H. and Carosi G. Turbulent time and length scale measurements in high-velocity open channel flows. *Experiments in Fluids*, 2007, **7**, No. 6, 495–508.
11. Crowe C., Sommerfield M. and Tsuji Y. *Multiphase Flows with Droplets and Particles*. CRC Press, Boca Raton, USA, 1998.
12. Chanson H. Air–water flow measurements with intrusive phase-detection probes. Can we improve their interpretation? *Journal of Hydraulic Engineering,* 2002, **128**, No. 3, 252–255.
13. Kucukali S. and Chanson H. *Turbulence in Hydraulic Jumps: Experimental Measurements*. Division of Civil Engineering, The University of Queensland, Brisbane, Australia, 2007, Report No. CH62/07.
14. Chanson H. Air entrainment in two-dimensional turbulent shear flows with partially developed inflow conditions. *International Journal of Multiphase Flow*, 1995, **21**, No. 6, 1107–1121.
15. Gualtieri C. and Chanson H. Experimental analysis of Froude number effect on air entrainment in the hydraulic jump. *Environmental Fluid Mechanics*, 2007, **7**, No. 3, 217–238.